1			
2	An Enhanced Droplet-Based Liquid Microjunction Surface Sampling System		
3	Coupled with HPLC-ESI-MS/MS for Spatially Resolved Analysis		
4			
5	Vilmos Kertesz* ^{1,} Taylor M. Weiskittel ² , and Gary J. Van Berkel ¹		
6			
7	¹ Organic and Biological Mass Spectrometry Group		
8	Chemical Sciences Division, Oak Ridge National Laboratory		
9	Oak Ridge, TN 37831-6131		
10 11	² ORISE HERE Intern, University of Tennessee, Knoxville, TN 37996		
12	ONISE HEINE IIILEIII, Oliversity of Termessee, Mioxville, TN 37990		
13			
14	Submitted for publication in special issue highlighting Mass Spectrometry Imaging in		
15	Analytical and Bioanalytical Chemistry		
16			
17	*Corresponding author		
18	VK: 865-574-3469		
19	Fax: 865-576-8559		
20	Email: kerteszv@ornl.gov		
21			
22	Running Title: Improvements in LMJ/HPLC/MS		
23	Figures: 4		
24	Schemes 1		
25	Supplemental Figures: 8		
26	Supplemental Tables: 5		
27	Supplemental Schemes: 1		
28			
29	This manuscript has been authored by a contractor of the U.S. Government under contract DE-AC05-		
30	00OR22725. Accordingly, the U. S. Government retains a paid-up, nonexclusive, irrevocable, worldwide		
31	license to publish or reproduce the published form of this contribution, prepare derivative works, distribute		
32	copies to the public, and perform publicly and display publicly, or allow others to do so, for U.S.		
33	Government purposes.		
34			

Abstract

35

36

37

38

39

40

41

42

43

44

45

46

47

48

49

50

51

52

53

54

Droplet-based liquid microjunction surface sampling coupled with HPLC-ESI-MS/MS for spatially resolved analysis provides the possibility of effective analysis of complex matrix samples and can provide a greater degree of chemical information from a single spot sample than is typically possible with a direct analysis of an extract. Described here is the setup and enhanced capabilities of a discrete droplet liquid microjunction surface sampling system employing a commercially available CTC PAL autosampler. The system enhancements include incorporation of a laser distance sensor enabling unattended analysis of samples and sample locations of dramatically disparate height as well as reliably dispensing just 0.5 µL extraction solvent to make the liquid junction to the surface the extraction spot size was confined to an area about 0.7 mm in diameter, software modifications improving the spatial resolution of sampling spot selection from 1.0 mm to 0.1 mm, use of an open bed tray system to accommodate samples as large as whole body rat thin tissue sections and custom sample/solvent holders that shorten sampling time to approximately 1 min per sample. The merit of these new features was demonstrated by spatially resolved sampling, HPLC separation, and mass spectral detection of pharmaceuticals and metabolites from whole body rat thin tissue sections and non-flat razor blade ("crude") cut mouse tissue.

Keywords: liquid microjunction, droplet-based liquid extraction, autosampler, spatial distribution, laser distance sensor

57

58

59

60

61

62

63

64

65

66

67

68

69

70

71

72

73

74

75

76

77

78

Introduction

Spatially resolved liquid-solid extractive sampling of surfaces combined with mass spectrometric analysis of the extracts using a continuous flow liquid microjunction surface sampling probe (CF-LMJ-SSP) was introduced in the early 2000's [1]. This sampling probe was designed to both continuously deliver a liquid extraction solvent to a surface forming a wall-less liquid junction between the probe and the surface and to aspirate away the solvent extract for immediate analysis by electrospray ionization (ESI) - or atmospheric pressure chemical ionization (APCI) - mass spectrometry (MS) [2]. Over the course of the last decade multiple continuous flow [1,2,3,4,5,6,7] as well as discrete droplet [8,9] variations of this liquid microjunction surface sampling and analysis approach have been implemented for numerous applications. The increased interest in this spatially resolved surface sampling/analysis methodology is due, in part, to the unrivaled sensitivity compared to other ambient surface sampling techniques [10,11], owing to the efficiency of analyte extraction. In addition, some of these liquid microjunction probe/methods allow ready transfer of the sampled material for postsampling processing, such as a high performance liquid chromatography (HPLC) separation, prior to mass spectral analysis [5,9,12,13,14]. Such a configuration enables effective analysis of targeted analytes within complex matrices well as the ability to differentiate isobaric compounds, thus providing a greater degree of chemical information from a single spot sample than is possible with a direct analysis.

With respect to discrete droplet liquid microjunction surface sampling, our group first implemented and continues to advance a system combined with HPLC-MS that

80

81

82

83

84

85

86

87

88

89

90

91

92

93

94

95

96

97

98

99

100

101

utilizes a widely available (CTC PAL) commercial autosampler [9,12,13,14]. This is a standalone system that connects to the existing liquid introduction ionization source (e.g. ESI or APCI) of the mass spectrometer. With this system, sampling is commenced by drawing a predefined amount of extraction solvent from a vial into the autosampler syringe needle (sampling probe) and barrel, followed by switching the needle configuration into surface sampling mode (needle protruding over the needle guide). As illustrated in sections II-V of Figure 1b, the syringe needle is then positioned at a predefined distance (100-300 µm in general) above a defined surface spot (Figure 1b, II) and a discrete volume of extraction solvent is dispensed onto a surface creating a liquid junction between the needle and the surface (Figure 1b, III). After a predefined extraction time (Figure 1b, IV), the liquid is drawn back into the syringe needle (Figure 1b, V), followed by switching the needle configuration from surface sampling mode to injection mode (needle leveled with the needle guide), and the analyte transferred to an injector and injected for subsequent chromatographic separation and mass spectral analysis. We have used this instrumentation and various operational methods to determine the spatially resolved, semi-quantitative, distribution of pharmaceuticals and metabolites in mouse and rat thin tissues sections [9,12,13].

During the course of these prior studies, some experimental and practical limitations were identified for improvement. For example, spot sampling size was approximately 1 mm (defined by the diameter of the probe to surface liquid junction), but was limited by software to selected locations on the nodes of a grid with a 1 mm node-to-node distance. This inhibited precise selection of sampling location. Studies found that reliable spot sampling required an optimum probe to surface distance with a

relatively tight tolerance [14]. To remain within this optimum range, the sample height could not vary by more than about 0.2 mm across the surface to be analyzed [14]. Inhomogeneity in sample height due to tilting of the autosampler tray holding the sample or due to the typical double-sided tape mounting of the tissue to a glass slide could easily cause a 0.2 mm variation or more. This fact limited the ability to easily setup and to automatically analyze tissue or any other samples of disparate height. In addition, the overall sample size was limited to what could be placed on a single microliter plate area. For example whole body mice tissue could be analyzed [9], but rat tissues had to be cut in half and analyzed as two separate samples.[12,13] And finally, extraction solvent vial and sample locations resulted in time consuming, complicated and long-distance robot movements resulting in a sampling time of about 1.7 min. This lengthy time could limit sample throughput if fast chromatographic separations are implemented.

In this paper, we report on the latest enhancements to our discrete droplet liquid microjunction surface sampling system that overcome these prior deficiencies. These enhancements include incorporation of a laser distance sensor enabling unattended analysis of samples and sample locations of dramatically disparate height, software modifications improving the spatial resolution of sampling spot selection from 1.0 mm to 0.1 mm, use of an open bed tray system to accommodate samples as large as whole body rat thin tissue sections and custom sample/solvent holders that shorten sampling time by about 40% to approximately 1 min per sample. The merit of these new features was demonstrated by spatially resolved sampling, HPLC separation, and mass spectral

detection of pharmaceuticals and metabolites from whole body rat thin tissue sections and non-flat razor blade ("crude") cut mouse tissue.

Experimental

Reagents

Chemicals. LC-MS grade Chromasolv® solvents 100/0.1 (v/v) water/formic acid (FA) and 100/0.1 (v/v) acetonitrile (ACN)/FA were obtained from Sigma Aldrich (St. Louis, MO, USA). Propranolol hydrochloride (compound **1** in Scheme 1, Acros Organics, Morris Plains, NJ, USA) and acetaminophen (Sigma Aldrich) were obtained commercially and used without further purification. Proprietary drug compound AZ-3 (>98% purity) was provided by AstraZeneca Pharmaceuticals (Waltham, MA, USA).

Rat Thin Tissue Sections. Male rats (HanWistar, 150-225 g) were dosed orally at a level of 40 mg/kg and 100 mg/kg with propranolol and acetaminophen, respectively. The dosed rats were sacrificed 2 h or 1 h after dose, respectively, using isoflurane anesthesia followed by freezing in a -80 °C dry ice/hexane bath. The frozen carcasses were embedded on a microtome mold/stage in an ice-cold aqueous solution of 2% carboxymethylcellulose for 1 h. The stages were then transferred to a -20 °C freezer for a night. Once frozen, five sagittal whole-body cryosections (40 μm thick) at different level of interest were prepared using a cryomicrotome (model Vibratome, Leica Microsystems GmbH, Wetzlar, Germany). Frozen sections were transferred to a one-sided adhesive tape. Tissue sections were stored at -20 °C until analysis. Just prior to analysis. samples were taken out from the freezer and allowed to come to room

temperature in a desiccator. While the impact of thawing on spatial distribution of the analytes of interests was not evaluated, negligible redistribution of drug and metabolites can be expected due to the use of a desiccator.

Mouse Tissue Sections. Nude NCR mice (n=3) were dosed subcutaneously with 111 μmol/kg (50 mg/kg) of AZ-3 and sacrificed after 2 h for necropsy, in which liver and muscle tissue were removed and snap-frozen (dry-ice and isopentane). A control group (n = 3) received no compound dose, where necropsy and tissue preparation methods were identical. Tissue slices were taken manually by a sharp razor blade and thaw-mounted onto glass microscope slides, which were stored at −80°C until required. Just prior to analysis, samples were taken out from the freezer and allowed to come to room temperature in a desiccator.

Custom Sample Trays. Custom sample holders, microtiter plate and double width microtiter plate size (Figures 1a and S1), were designed in AutoCad 2015 (Autodesk, Inc., San Rafael, CA). All holders included a recessed sample region, space for 4 individual extraction solvent vials and a smaller diameter hole used in locking the needle guide to assist with switching the injector needle configuration into surface sampling mode [12,13]. Multiple trays were printed at 0.3 mm layer thickness using either polylactic acid (PLA) or acrylonitrile butadiene styrene (ABS) plastics using either a Solidoodle 3rd generation (Solidoodle LLC, Brooklyn, NY) or a Fortus 900 mc (Stratasys, Eden Prairie, MN) 3D printer.

Surface Sampling/HPLC Instrumentation and Operation. The work described herein utilized an HTS-PAL autosampler (LEAP Technologies Inc., Carrboro, NC) equipped with a 100-μL L-MARK[®] 22s-gauge gastight syringe with a fixed needle (part

171

172

173

174

175

176

177

178

179

180

181

182

183

184

185

186

187

188

189

190

191

192

no: LMK- 2620719, 152 μm i.d., 717 μm o.d., LEAP Technologies Inc.) and an API 4000™ triple quadrupole mass spectrometer (AB SCIEX, Concord, Ontario, Canada). Communication control and data flow between the instruments are illustrated in supplemental Figure S2. The autosampler system and setup was similar to that described previously [12,13,14]. Changes included addition of a laser distance sensor (model ZX2-LD100, Omron, Hoffman Estates, IL) mounted on the autosampler, use of custom 3D printed sample holders (see above), and an open sample tray holder (model PAL.TRHLDLC, LEAP Technologies Inc., see Figure 1a) rather than the previously used cool stack [12,13,14]. Samples were mounted in the recess of the custom trays using double sided tape. The tray with the mounted sample was coupled with a 3D printed "tray riser" (not shown), that raised the sample off the surface of the flatbed scanner (model Perfection v300 Photo, Epson America Inc., Long Beach, CA, USA) used to obtain an optical image of the surface to be analyzed for software guided selection of sampling locations using in-house developed software (LMJ Points Plus[©]) [12,13,14]. The procedure for selection of sampled positions and co-registration of the optical image to these positions were similar to that previously described elsewhere [12,13,14] with the difference that locations could be selected with 0.1 mm precision rather than the previous limit of 1 mm.

Once the surface locations were selected for analysis in LMJ Points Plus[©], the user transferred this information into LEAPShell 3TM (LEAP Technologies Inc) controlling the autosampler via a text file imported into the sample queue of the software. The autosampler method assigned to the queue positioned the laser distance unit above a surface location to be sampled (Figure 1b, I) followed by sending out a TTL

194

195

196

197

198

199

200

201

202

203

204

205

206

207

208

209

210

211

212

213

214

215

signal on one digital output of the autosampler. This signal was sensed by LMJ Points Plus[©] via a digital input port of a USB-1208LS data acquisition device (Measurement Computing, Norton, MA, USA) that triggered the measurement of the laser sensor-tosurface distance using the laser distance sensor mounted on the autosampler vertical arm. These distances were collected in the sample list in LMJ Points Plus[©] and they were later used for correct positioning of the autosampler syringe needle along the vertical Z-axis to ensure a proper distance between the sampling device and the surface during surface sampling (see detailed discussion below). Once the sample gueue was completed, the user transferred the surface locations to be analyzed along with distance information collected above from LMJ Points Plus[©] into LEAPShell 3TM again via a text file imported into the sample queue of the latter software. In addition, the required HPLC/MS acquisition method and MS data file names were also transferred into Analyst[™] (AB SCIEX) via a third text file to create an Analyst[™] sample queue. Serial sampling of previously selected locations was commenced in LEAPShell 3TM. Samples were injected onto a Hydro-RP HPLC column (50 x 2 mm, 4um particle size; Phenomenex, Torrance CA) for subsequent HPLC-ESI-MS/MS analysis employing an Agilent 1100 HPLC pump (Agilent Technologies, Santa Clara, CA) to deliver the separation solvents coupled to an API 4000 triple quadrupole mass spectrometer (AB SCIEX). HPLC separation solvents A and B were 100/0.1 (v/v) water/FA and 100/0.1 (v/v) ACN/FA, respectively. HPLC separation conditions are listed in Table 1 for all samples. Solution flow rate was 200 µL/min for all experiments. Selected reaction monitoring (SRM) was used to monitor all compound of interest. Mass spectrometric conditions including electrospray ionization (ESI) mode, emitter voltage (IS), monitored

precursor (Q1) and fragment (Q3) masses, collision energy (CE) and declustering potential (DP) are listed in Table 2. Dwell time was 50 ms for each transition monitored. Turbo sprayer heater temperature was 400 °C.

219

216

217

218

220

221

222

223

224

225

226

227

228

229

230

231

232

233

234

235

236

237

238

Results and Discussion

Laser Distance Sensing for Analysis of Samples and Sample Locations of **Disparate Height.** To reliably and automatically position the sampling probe the proper distance above a sample for solvent dispense and aspiration, a laser distance sensor was attached to the vertical arm of the robotic autosampler (Figure 1). Following selection of the sampling locations with the LMJ Points Plus® software, as described in the Experimental Section the robot arm was moved automatically to position the laser sensor sequentially above each selected location where the laser sensor-to-surface distance was measured (Figure 1b, I). Using this measured distance (D) and a previously determined vertical offset (D_f) between the laser sensor and the probe (tip of the autosampler syringe needle), the actual probe-to-surface distance ($D_z = D - D_f$) was calculated in LMJ Points Plus $^{\odot}$. This D_z distance was then used to calculate how far the probe needed to move down vertically during the sampling process (D_z - d_0 , Figure 1b, II) at the specific spot to obtain the predetermined optimal d_0 (0.2 mm in the current study) probe-to-surface distance. The actual surface sampling commenced after all these distance measurements were completed. For each sampling location the autosampler first drew 5 µL of extraction solvent from a vial in one of the vial holders (indicated by "2" in Figure 1a) located on the custom sample tray. This was followed by

240

241

242

243

244

245

246

247

248

249

250

251

252

253

254

255

256

257

258

259

260

261

switching the syringe needle configuration into surface sampling mode using the needle lock hole (indicated by "1" in Figure 1a) also located on the custom sample tray. As illustrated in Figure 1b (II), this step was followed by moving the probe to the optimal d_0 sampling distance from the surface and a specific volume of extraction solvent (see Table 1) was dispensed onto the selected surface spot of interest creating a liquid junction (Figure 1b, III). After a given extraction time (Figure 1b, IV and Table 1), the solvent with sample was aspirated back into the syringe (Figure 1b, V) and the full 5 μ L sample was injected onto an HPLC column for subsequent HPLC-ESI-MS//MS analysis.

The data in Figure 2 illustrates the results of this laser distance sensing and automated analysis using a whole body rat thin tissue section from an animal dosed with propranolol (40 mg/kg P.O., sacrificed 2 h post dose). The 30 surface locations analyzed (marked with plus signs in Figure 2a) were expected to exhibit well-defined distributions of the parent drug and its metabolites demonstrating the analytical power of the current method and should not be construed to suggest that these compounds were not distributed to other tissues. The areas selected for analysis included embedded blood spots spiked with different propranolol concentrations (0 to 5000 ng/mL, see Figure 2b), parts of the brain, lung, heart (muscle and blood), liver, intestinal lining, rectum and testis. The spots sampled by using 2 µL of 90/10/0.1 (v/v/v) water/ACN/FA encompassed an area of approximately 156.4 mm x 40.4 mm in size. Over this area, the surface heights were measured to differ by as much as 1.3 mm between some locations as illustrated by the height difference measurements shown for each spot compared to the unspiked embedded blood sample location (Figure 2a). automated adjustment of the probe positioning between sampling locations, analysis

263

264

265

266

267

268

269

270

271

272

273

274

275

276

277

278

279

280

281

282

283

284

would have been unsuccessful for any location with a height variation of more than about 0.2 mm compared to this reference point. Visual inspection during the analysis process confirmed in this case that sampling from all 30 locations was successful despite the significant height variations between the sampled spots.

From the data collected at each sample location on the tissue section, compound specific abundances of propranolol and two hydroxypropranolol glucuronide metabolites were determined using a procedure described previously [12,13,14]. Briefly, LMJ Points Plus[©] software was provided with filenames and retention time ranges for background and peak area calculation for these compounds. In Figure 2d, the white and gray sections between R_t =2-2.5 min and R_t =4.6-5.1 min represent the ranges where background signal was sampled and from which background-corrected peak area for propranolol (R_t =4.7 min) was calculated, respectively. Similarly, white and gray sections between R_t =2-2.5 min and R_t =4.2-4.5 min in Figure 2e indicate retention time ranges from which peak area for aliphatic hydroxypropranolol glucuronide metabolites (cpd **1b** in Scheme 1, R_t =4.3 min) was calculated. (Note, that spatial distribution profiles and relative abundances for both hydroxypropranolol glucuronide metabolites, i.e., cpds 1a (see Scheme 1) and 1b, in all areas of the tissue section were found to be very similar [9]. For that reason the discussion of metabolite results is limited to the aliphatic hydroxypropranolol glucuronide metabolite.) Integrated HPLC-ESI-MS/MS peak areas for the parent drug and the metabolite are presented in Figures 2b and c, respectively, as circles with a false color scale (heat maps). The diameter of the circles was set to the liquid junction diameter (about 2 mm) at the various sampling locations. In this case, a logarithmic intensity color scale was used to reflect the relative integrated

HPLC-ESI-MS/MS peak areas measured [12]. The heat maps for the spiked blood indicated that there was an increase in signal for propranolol with increased spike level (Figure 2b). Plotting the peak area of propranolol as a function of its spiked concentration for these blood samples showed a linear relationship (Figure S3) proving that the analytical results observed are expected to be at least semiquantitative. In addition, spatial distribution profiles presented in Figure 2b and c for the parent drug and metabolite, respectively, were in agreement with those observed previously using various liquid extraction based surface sampling methods to analyze tissues of mice dosed following a similar dosing protocol as described here [8,9,15,16], and using tissues made from the same animal [12]. Only the parent drug was found in the brain and the intestinal lining exhibited both the parent drug and the metabolite in the largest amounts.

An additional benefit not obvious from just the displayed data is the time savings accrued by the use of the custom sample and vial holder. This change in the system reduced the sampling process from about 1.7 min [12,13,14] by about 40% to 1 min per sample. Over the course of the analysis of the 30 samples, that savings equated to about 20 min or a 10 % reduction in analysis time, which was ultimately limited by the 6 min chromatography currently employed.

Sample Location Selection Spatial Resolution. The spatial resolution of sample spot selection was improved from 1.0 mm to 0.1 mm with this version of our system. This enabled the ability to sample much more precisely specific locations on a surface.

In a previous study, we observed the sulfate metabolite of acetaminophen (cpd 2 in Scheme 1) in the small gastrointestinal tract and what appeared to be in a vein in the liver, but not in the bulk liver tissue from a rat dosed with acetaminophen (100 mg/kg P.O., sacrificed 1 h post dose) [13]. That observed distribution was likely due to hepatic metabolism and biliary excretion of acetaminophen sulfate into the small intestine. Unfortunately the 1.0 mm precision of spot selection available in that study limited exact sampling from the small size veins visible in the liver.

Figure 3a shows an optical image of a rat thin tissue section from the same rat used in that prior study with portions of the liver, spine and lung visible. Evident within the liver are the locations of several veins. The zoomed in image in Figure 3b, corresponds to one of these veins marked by a black rectangle in Figure 3a. Superimposed on this image of the roughly 1 mm wide X 4 mm long tear drop shaped vein are 25 white crosses showing the surface locations selected for sampling. The ability to select the sampling location with 0.1 mm precision allowed for selection of sampling locations centered in the 1.0 mm wide feature of interest. The remaining locations were on the nodes of a 5 x 5 grid with 0.5 mm spacing and were picked to include surface locations located both in the bulk liver tissue and as well as in the vein. By dispensing just 0.5 μ L of 90/10/0.1 (v/v/v) water/ACN/FA extraction solvent to make the liquid junction to the surface the extraction spot size was confined to an area about 0.7 mm in diameter (the outer diameter of the syringe needle), justifying the close sample location spacing.

The spatial distribution linear intensity heat map for acetaminophen sulfate determined from the HPLC-ESI-MS/MS data (Figure S4 in the *Supplemental section*) at

these sampling locations is shown in Figure 3c. These data confirm that the distribution of the sulfate metabolite was restricted to the vein region of the liver tissue.

Analysis of Razor Blade ("Crude") Cut Tissue Sections. Crude cut or biopsy tissue represent other types of tissues that might be prepared for analysis that are of disparate height. The size of these tissue can also be relatively small (e.g., 1 mm width) such that spot selection with a precision of 0.1 mm is required for effectively sampling. Figure 4a shows an optical image of crude cut muscle and liver bulk tissues harvested from both a non-dosed mouse and a mouse dosed with AZ-3 (50 mg/kg, dosed subcutaneously, sacrificed 2 h after dose). Sampling locations are indicated in the figure by black crosses with the relative height differences among the sampling points also indicated (Figures S5a-d in the *Supplemental section* present magnified views of the samples.). While some of the sampling locations differed in height by as much as 1.9 mm, and some samples as narrow as 1 mm, all locations were sampled successfully by using 4 µL of 50/50/0.1 (v/v/v) water/ACN/FA.

The relative amount of AZ-3 in the different tissue samples analyzed was determined from the chromatographic peak areas (Figure S5e in the *Supplemental section*) and is displayed as a linear intensity heat map in Figure 4b. Based on data obtained in the previous study [17], it was expected and the data here confirmed that liver from dosed animal exhibited significantly larger amount of AZ-3 than muscle tissue from the same specimen. Calculated relative liver-to-muscle ratio of parent drug was 4.9 (±3.3). This ratio was somewhat lower than the ratio of 9.13 obtained from HPLC-ESI-MS/MS analysis of tissue homogenates and of 9.5 (±2.2) from direct liquid microjunction/ESI-MS/MS based sampling of thin tissues [17] This difference could be

due in part to the aging of the samples (>5 years storage of samples used for measurements in [17]) or the fact that the current method analyzed the surface of a bulk tissue while HPLC-ESI-MS/MS analysis used a tissue homogenate and the previously employed surface sampling method utilized a thin tissue section. Nonetheless, the present results demonstrate the first time that reliable sampling of crude cut bulk tissue samples can be accomplished by the current automated setup to provide semi-quantitative data on exogenous analyte content.

Conclusion

In this paper we described the setup and capabilities of our discrete droplet liquid microjunction surface sampling system employing a commercially available CTC PAL autosampler. Addition of a laser distance sensor provided unattended analysis of samples and sample locations of dramatically disparate height, software modifications improving the spatial resolution of sampling spot selection from 1.0 mm to 0.1 mm, open bed tray system and custom sample/solvent holders allowed samples as large as whole body rat thin tissue sections that shorten sampling time by about 40%. These new features were demonstrated by spatially resolved sampling, separation, and detection of propranolol and its phase II metabolite hydroxypropranolol glucuronide, and phase II metabolite acetaminophen sulfate from whole body rat thin tissue sections, and a proprietary drug (AZ-3) from non-flat razor blade cut "crude" organs from drug dosed mice.

Two further improvements are envisioned for the near future. One of them focuses on integrating the control of the autosampler into LMJ Points Plus® to enable sampling of a surface location right after its height is determined eliminating any complications associated with time dependent height changes. The other area of focus targets reliable quantitation. This analysis approach currently only provides a relative quantitative distribution of the analyte of interest. The signal observed for a compound does not reflect the absolute amount of material present at a given location. The incorporation of internal standards to compensate for matrix-specific suppressive effects and instrument response, maximizing analyte recovery from various surface types along with calibration curves employing suitable matrices are key aspects that are under investigation. The ability to accurately determine the concentrations of spatially distributed drugs and metabolites in tissue from small animal models and/or clinical samples will be of significantly more utility than semi-quantitative data.

Acknowledgements

The API 4000 instrument used in this work was provided on loan and advancement of this surface sampling technology was supported by funding provided through a Cooperative Research and Development Agreement (CRADA NFE-10-02966) with AB Sciex. Drs. Jimmy Flarakos, Paul Moench, Adam Bentley and Alexandre Catoire (Novartis Pharmaceuticals Corporation, East Hanover, NJ) are thanked for providing the whole-body rat thin tissue sections through a Work for Others (WFO) agreement with Novartis Institutes for Biomedical Research. AstraZeneca

Pharmaceuticals (Waltham, MA, USA) is thanked for providing the AZ-3 dosed mouse tissues through a WFO agreement. T.M.W. acknowledges an ORNL appointment through the ORISE HERE program that was supported through the WFO agreement with Novartis Institutes for Biomedical Research. The authors would like to thank Lonnie J. Love from the Manufacturing Demonstration Facility of the Oak Ridge National Laboratory for his valuable help in 3D printing of the custom trays.

Scheme 1. Structure, mass-to-charge ratio, and origin of major product ions for propranolol (1), hydroxypropranolol glucuronide metabolites (1a and 1b) and acetaminophen sulfate (2).

 Table 1. HPLC and extraction conditions employed for the samples analyzed. Solvents A and B correspond to water with 0.1% formic acid (FA) and to acetonitrile (ACN) with 0.1% FA, respectively. Only the percentage of solvent A is denoted in the table. The percentage of solvent A changes linearly in each step listed.

Sample	HPLC gradient program	Extraction solvent and volume	Extraction time (s)
Rat dosed with propranolol	0-0.5 min: 90% 0.5-3 min: 90% to 35% 3-3.5 min: 35% to 10% 3.5-3.6 min: 10% to 90% 3.6-6 min: 90%	2 μL of 90% A	2
Rat dosed with acetaminophen	0-0.5 min: 90% 0.5-1 min: 90% to 35% 1-2 min: 35% to 10% 2-2.1 min: 10% to 90% 2.1-5 min: 90%	0.5 μL of 90% A	5
Mouse dosed with AZ-3	0-0.5 min: 90% 0.5-3 min: 90% to 35% 3-3.5 min: 35% to 10% 3.5-5 min: 10% to 10% 5-5.1 min: 10% to 90% 5.1-8 min: 90%	4 μL of 50% A	2

Table 2. Selected reaction monitoring (SRM) conditions employed including electrospray ionization (ESI) mode, emitter voltage (IS), monitored precursor (Q1) and fragment (Q3) masses, collision energy (CE) and declustering potential (DP)

Sample	Monitored compound	ESI mode	IS (kV)	Q1/Q3 (m/z)	CE (V)	DP (V)
Rat dosed with	cpd 1	+	4.8	260.1/116.1	25	60
propranolol	cpd 1b	+	4.8	452.1/276.1	35	60
Rat dosed with acetaminophen	cpd 2	-	-4	232.1/150.1	-25	-75
Mouse dosed with AZ-3	AZ-3	+	4.5	452.2/172.1	42	130

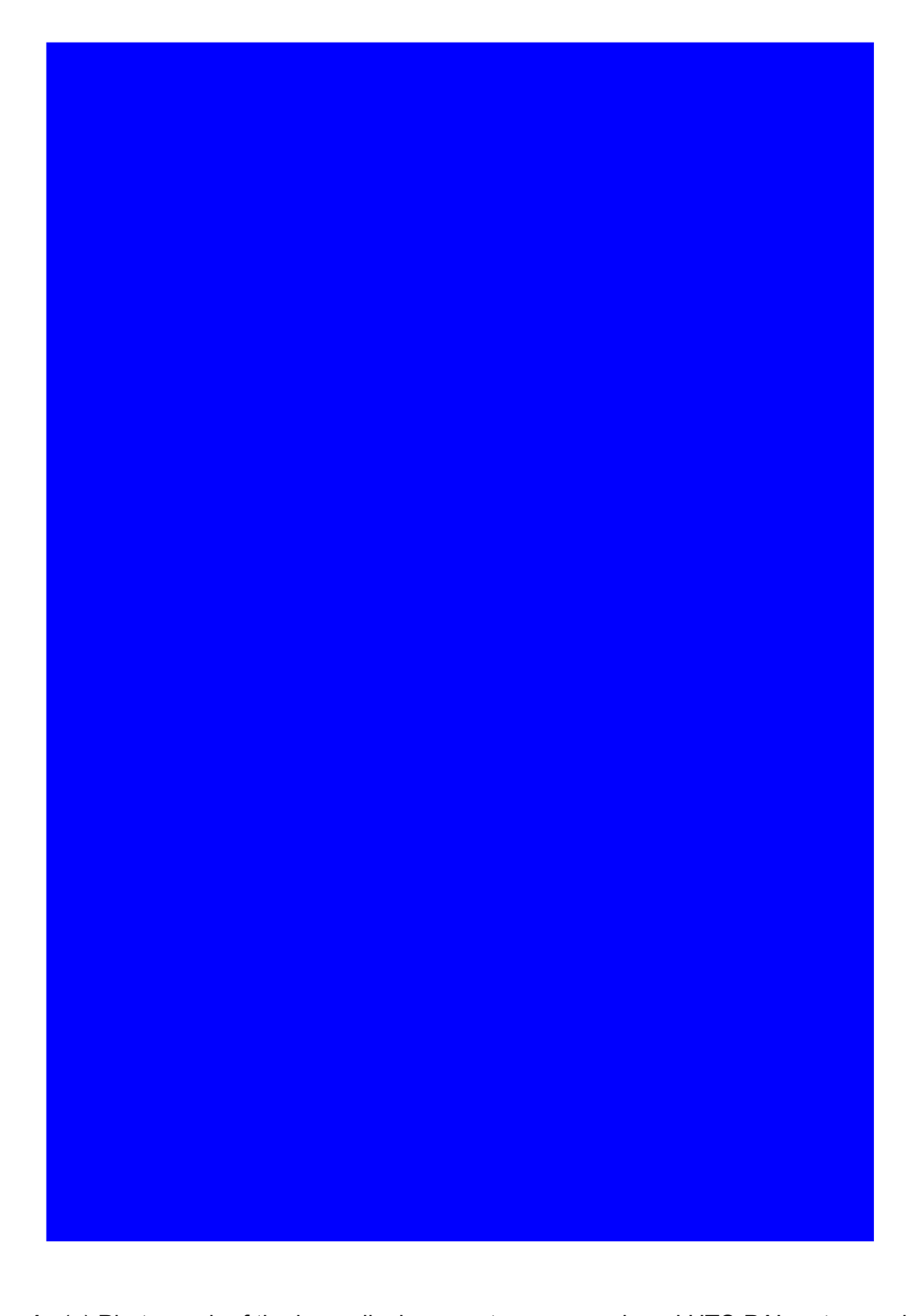


Figure 1. (a) Photograph of the laser displacement sensor equipped HTS-PAL autosampler hosting the 3D-printed large size sample holder with built-in hole to switch to surface sampling mode and a built-in 4-vial tray. Inset shows magnified view of left side of the 3D-printed sample

holder. (b) Schematic of the surface sampling process including (I) the positioning of the laser beam above a defined surface spot followed by the measurement of the laser sensor-to-surface distance (D) from which syringe tip-to-surface distance (D_z) is then calculated using a previously determined and fixed laser sensor-to-syringe tip distance (D_f), (II) the positioning of the syringe needle at a predefined distance (D_f) above the defined surface spot, (III) dispensing a discrete volume of extraction solvent onto a surface creating a liquid junction between the needle and the surface, (IV) dissolution of the analyte in the extraction solvent, and (V) the liquid is drawn back into the syringe needle after a predefined extraction time.

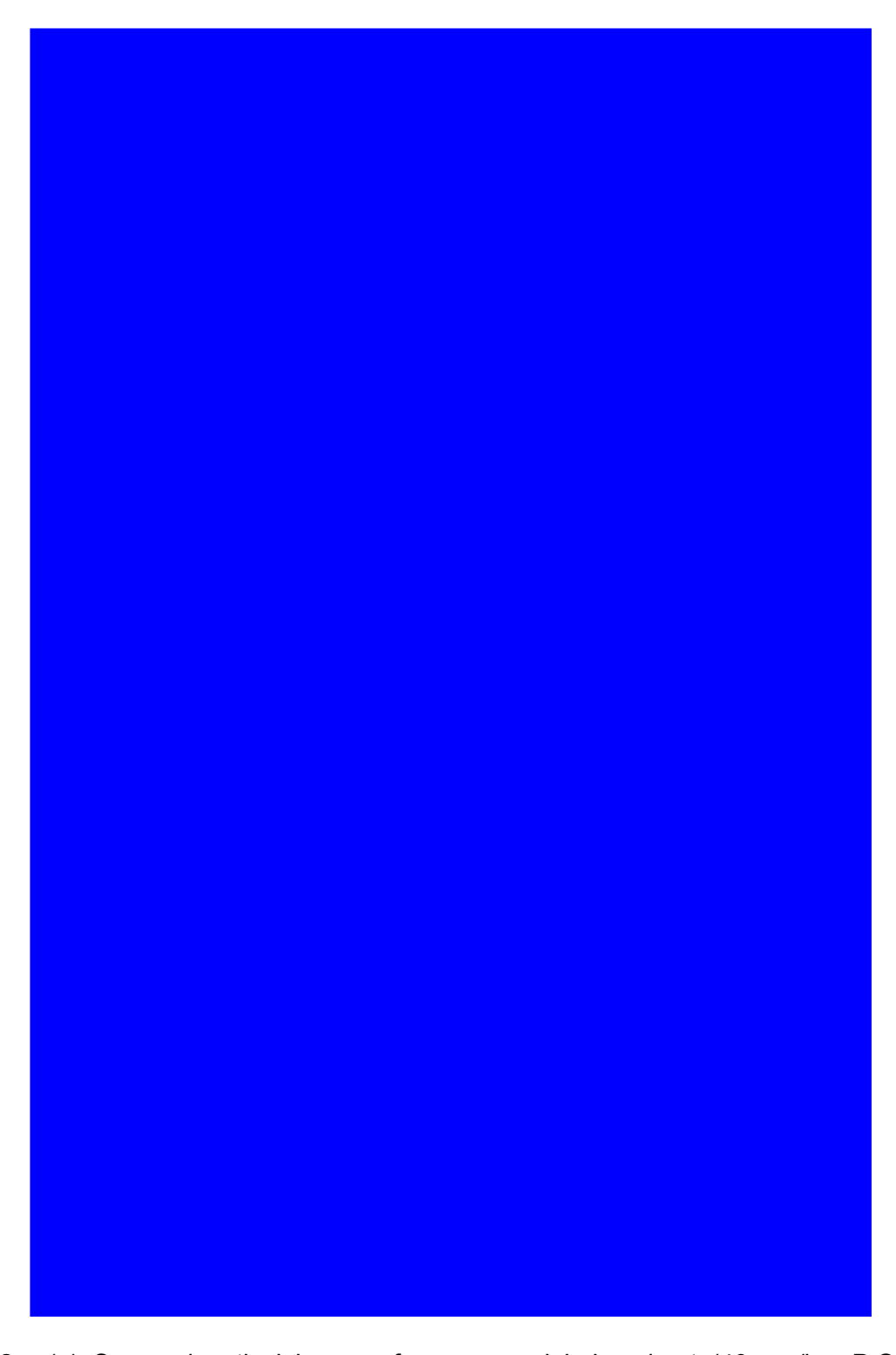


Figure 2. (a) Scanned optical image of a propranolol dosed rat (40 mg/kg, P.O. dosed, sacrificed 2 h after dose) whole-body thin tissue section on tape showing locations sampled and relative height difference in mm from the unspiked blood spot. Heat maps for cpds **1** and cpd **1b** are displayed in (b) and (c), respectively, with concentrations of cpd **1** in blood shown in (b).

The logarithmic intensity color scale used to create the two heat maps is shown in the bottom right corner of (c). 100% intensity corresponds to (b) 18.6 x 10^6 and (c) 25.6 x 10^6 counts, respectively. Chromatograms at the sampling spot indicated by the arrow in (b) recorded during a 6 min HPLC/MS analysis are shown for (d) propranolol (cpd $\mathbf{1}$, m/z 260.1 \rightarrow 116.1) and (e) hydroxypropranolol glucuronides (cpds $\mathbf{1a}$ and $\mathbf{1b}$, m/z 452.1 \rightarrow 276.1). Gray and white sections show the time ranges used for peak integration (R_t =4.6-5.1 min and R_t =4.2-4.5 min for cpds $\mathbf{1}$ and $\mathbf{1b}$, respectively) and background calculation (R_t =2-2.5 min for both cpds), respectively, when creating heat maps in (b) and (c), respectively.

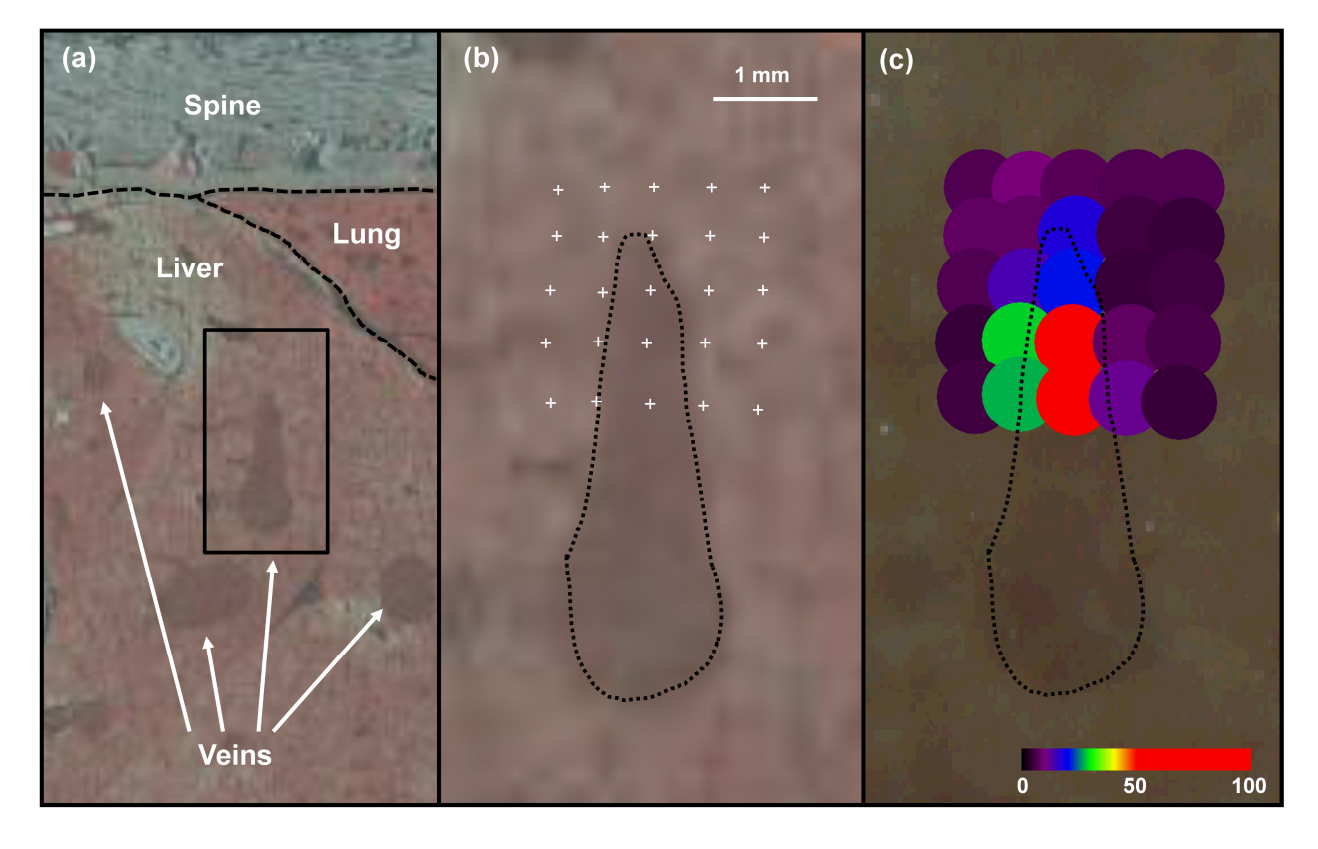


Figure 3. (a) Scanned optical images of an acetaminophen dosed rat (100 mg/kg, P.O. dosed, sacrificed 1 h after dose) whole-body thin tissue section on tape showing a blood vessel in liver (dotted line) (a) taken before sample shipment and (b) taken right before analysis showing the sampled surface locations (white crosses) and heat map of cpd **2** (peak: R_t =3-4 min, background: R_t =0.5-1 min). The linear intensity color scale used to create the heat map is shown in the bottom right corner. 100% intensity corresponds to 1.02 x 10⁵ counts.

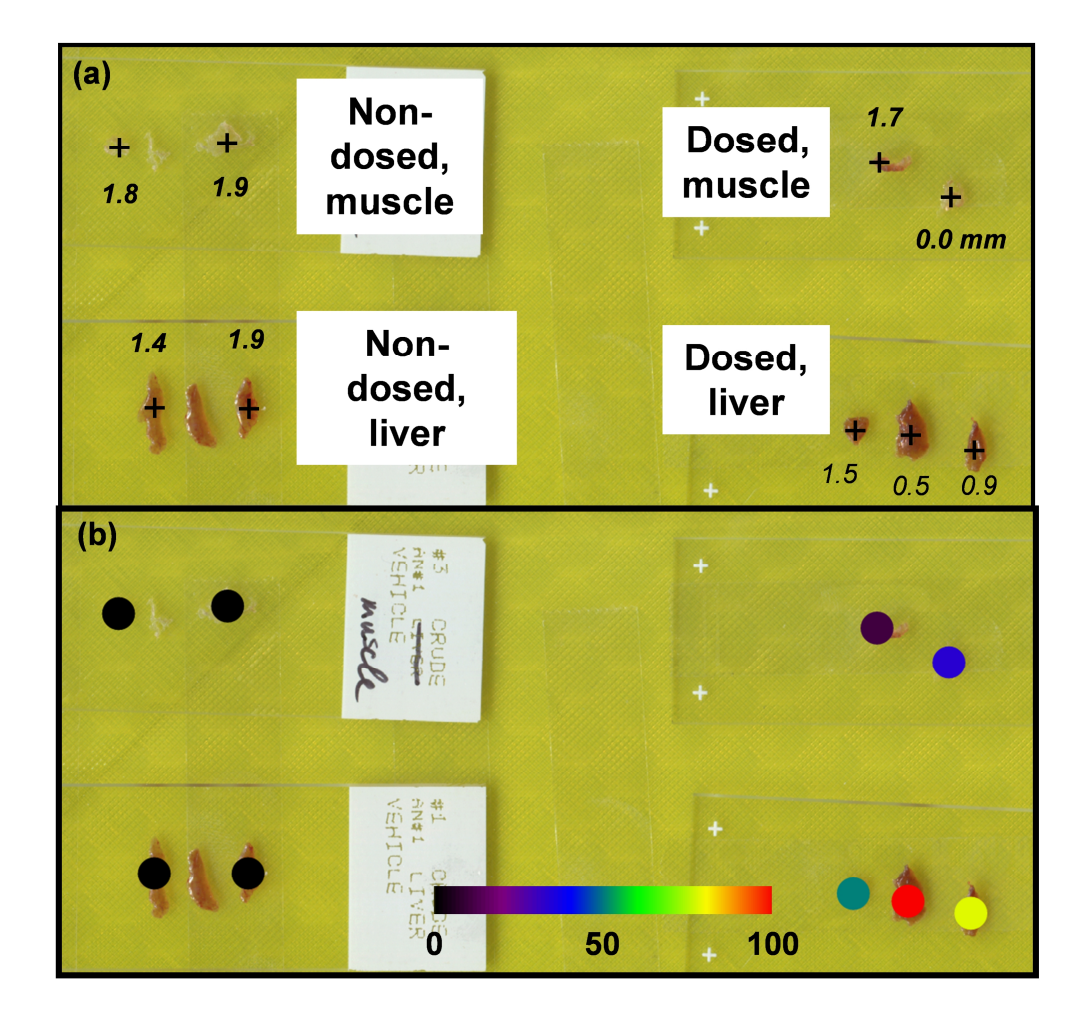


Figure 4. (a) Scanned optical image of muscle and liver samples of a non-dosed mouse and a mouse dosed with AZ-3 (50 mg/kg, dosed subcutaneously, sacrificed 2 h after dose) showing locations sampled (black crosses) and relative height differences in mm from one of the dosed muscle sample. (b) Heat map of cpd **AZ-3** (peak: R_t =5.3-5.8 min, background: R_t =1-1.5 min). The linear intensity color scale used to create the heat map is shown in the bottom section. 100% intensity corresponds to 7.50 x 10⁶ counts.

476 References

- 1. Van Berkel GJ, Sanchez AD, Quirke JME. (2002) Anal Chem 74:6216-6223
- 2. Asano KG, Ford MJ, Tomkins BA, Van Berkel GJ. (2005) Rapid Commun Mass Spectrom 19:2305-2312
- 3. Van Berkel GJ; Kertesz V, King RC.(2009) Anal Chem 81:7096-7101
- 4. ElNaggar MS, Barbier C, Van Berkel GJ. (2011) J Am Soc Mass Spectrom 22:1157-1166
- 5. Van Berkel GJ, Kertesz V. (2013) Rapid Commun Mass Spectrom 27:1329-1334
- 6. Roach PJ, Laskin L, Laskin A. (2010) Analyst 135:2233-2236
- 7. Momotenko D, Qiao L, Cortés-Salazar F, Lesch A, Wittstock G, Girault HH. (2012) Anal Chem 84:6630-6637
- 8. Kertesz V, Van Berkel GJ. (2010) J Mass Spectrom 45:252-260
- 9. Kertesz V, Van Berkel GJ. (2010) Anal Chem 82:5917-5921
- 10. Rao W, Celiz AD, Scurr DJ, Alexander MR, Barrett DA. (2013) J Am Soc Mass Spectrom 24:1927-1936
- 11. Montowska M, Rao W, Alexander MR, Tucker GA, Barrett DA. (2014) Anal Chem 86:4479-4487
- 12. Kertesz V, Van Berkel GJ. (2013) Bioanal 5:819-826
- 13. Kertesz V, Paranthaman N, Moench P, Catoire A, Flarakos J, Van Berkel GJ. (2014) Bioanal, in press
- 14. Kertesz V, Van Berkel GJ. (2014) Rapid Commun Mass Spectrom 28:1553–1560
- 15. Kertesz V, Van Berkel GJ, Vavrek M, Koeplinger KA, Schneider BB, Covey TR.(2008) Anal Chem 80:5168-5177
- 16. Van Berkel GJ, Kertesz V. (2009) Anal Chem 81:9146-9152
- 17. Blatherwick EQ, Van Berkel GJ, Pickup K, Johansson MK, Beaudoin M-E, Cole RO, Day JM, Iverson S, Wilson ID, Scrivens JH, Weston DJ. (2011) Xenobiotica 41:720-734

1	Supplemental Information			
2	An Enhanced Droplet-Based Liquid Microjunction Surface Sampling System			
3	Coupled with HPLC-ESI-MS/MS for Spatially Resolved Analysis			
4				
5	Vilmos Kertesz* ^{1,} Taylor M. Weiskittel ² , and Gary J. Van Berkel ¹			
6				
7	¹ Organic and Biological Mass Spectrometry Group			
8 9	Chemical Sciences Division, Oak Ridge National Laboratory Oak Ridge, TN 37831-6131			
10				
11 12	² ORISE HERE Intern, University of Tennessee, Knoxville, TN 37996			
13	Submitted for publication in special issue highlighting Mass Spectrometry Imaging in			
14	Analytical and Bioanalytical Chemistry			
15				
16				
17	*Corresponding author			
18	VK: 865-574-3469			
19	Fax: 865-576-8559			
20	Email: kerteszv@ornl.gov			
21				
22	Running Title: Improvements in LMJ/HPLC/MS			
23	Supplemental Figures: 5			
24				
25	This manuscript has been authored by a contractor of the U.S. Government under contract DE-AC05-			
26	00OR22725. Accordingly, the U. S. Government retains a paid-up, nonexclusive, irrevocable, worldwide			
27	license to publish or reproduce the published form of this contribution, prepare derivative works, distribute			
28	copies to the public, and perform publicly and display publicly, or allow others to do so, for U.S.			
29	Government purposes.			
30				



Figure S1. Photograph of 3D printed custom trays showing (top) microtiter plate sized ones and (bottom) one with double the width of a microtiter plate allowing to mount a full whole body rat thin tissue section.

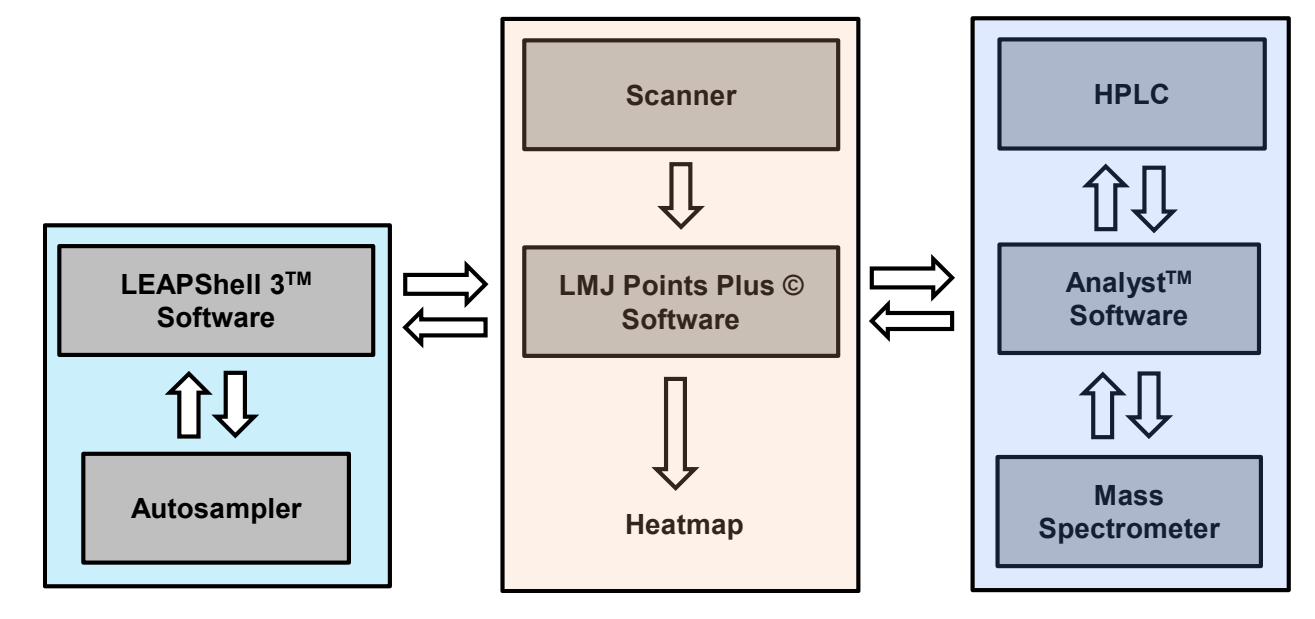


Figure S2. Workflow of the surface sampling system.

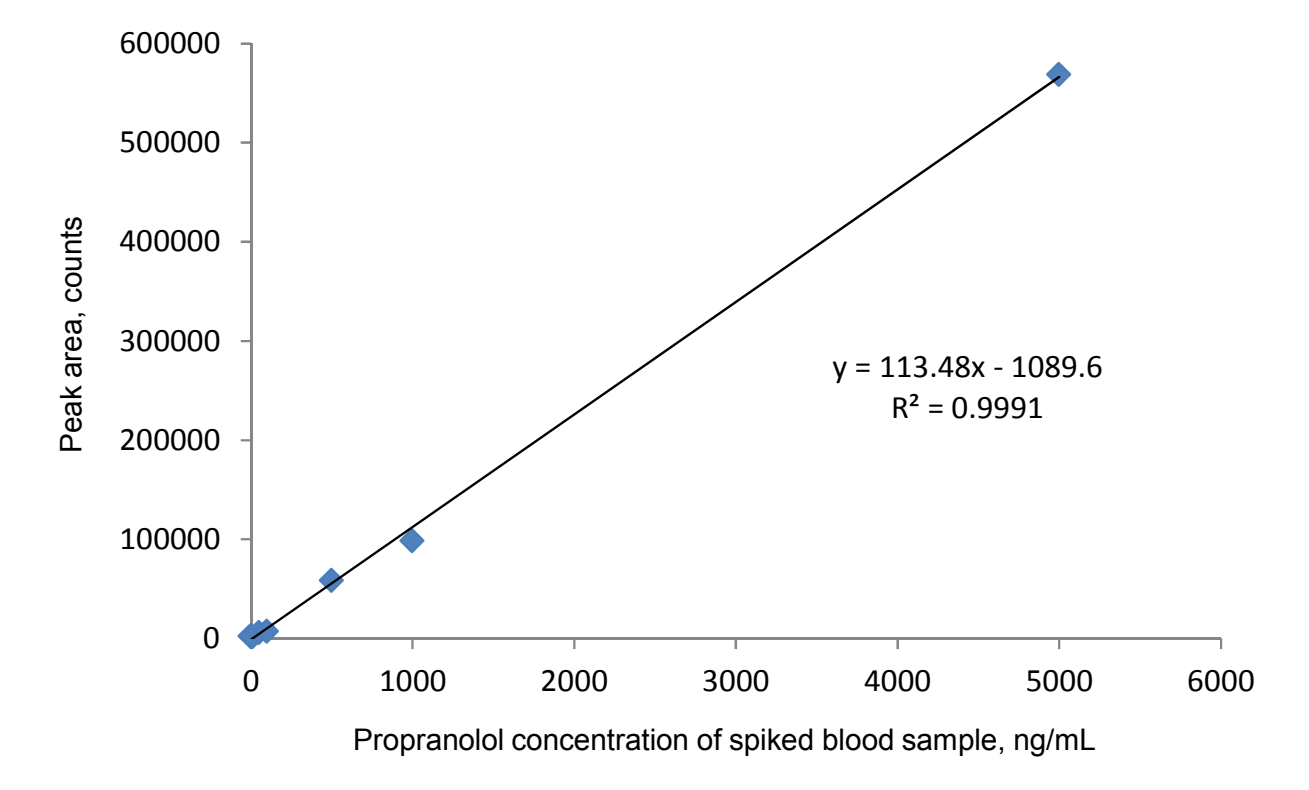
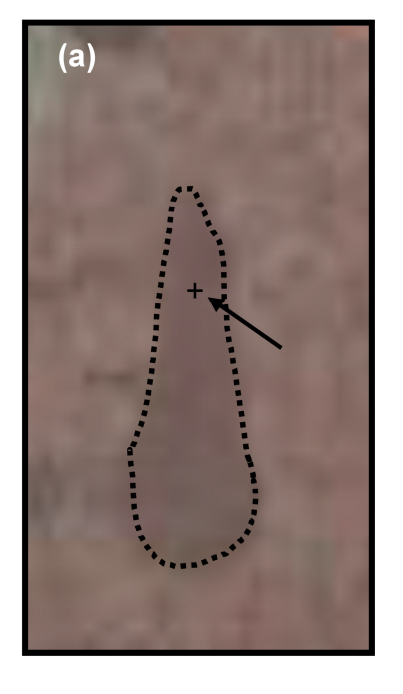


Figure S3. Peak area of propranolol as a function of its spiked concentration for blood samples shown in Figure 2.



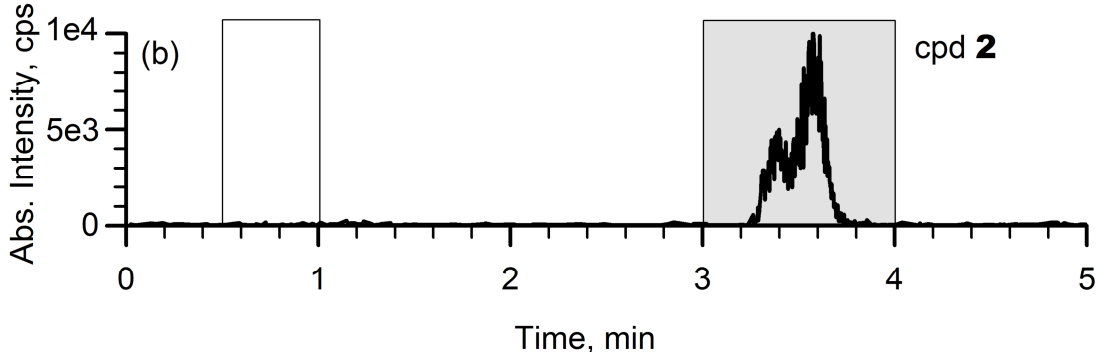


Figure S4. (a) Scanned optical image of an acetaminophen dosed rat (100 mg/kg, P.O. dosed, sacrificed 1 h after dose) whole-body thin tissue section on tape showing a sampled location indicated by the arrow and the "+" sign. (b) Signal level at this sampling spot was recorded during a 5 min HPLC/MS analysis for acetaminophen sulfate (cpd **2**, m/z 232.1 \rightarrow 150.1). Gray and white sections show the time ranges used for peak integration (R_t =3-4 min) and background calculation (R_t =0-0.5 min), respectively, when creating a heat map in Figure 3.

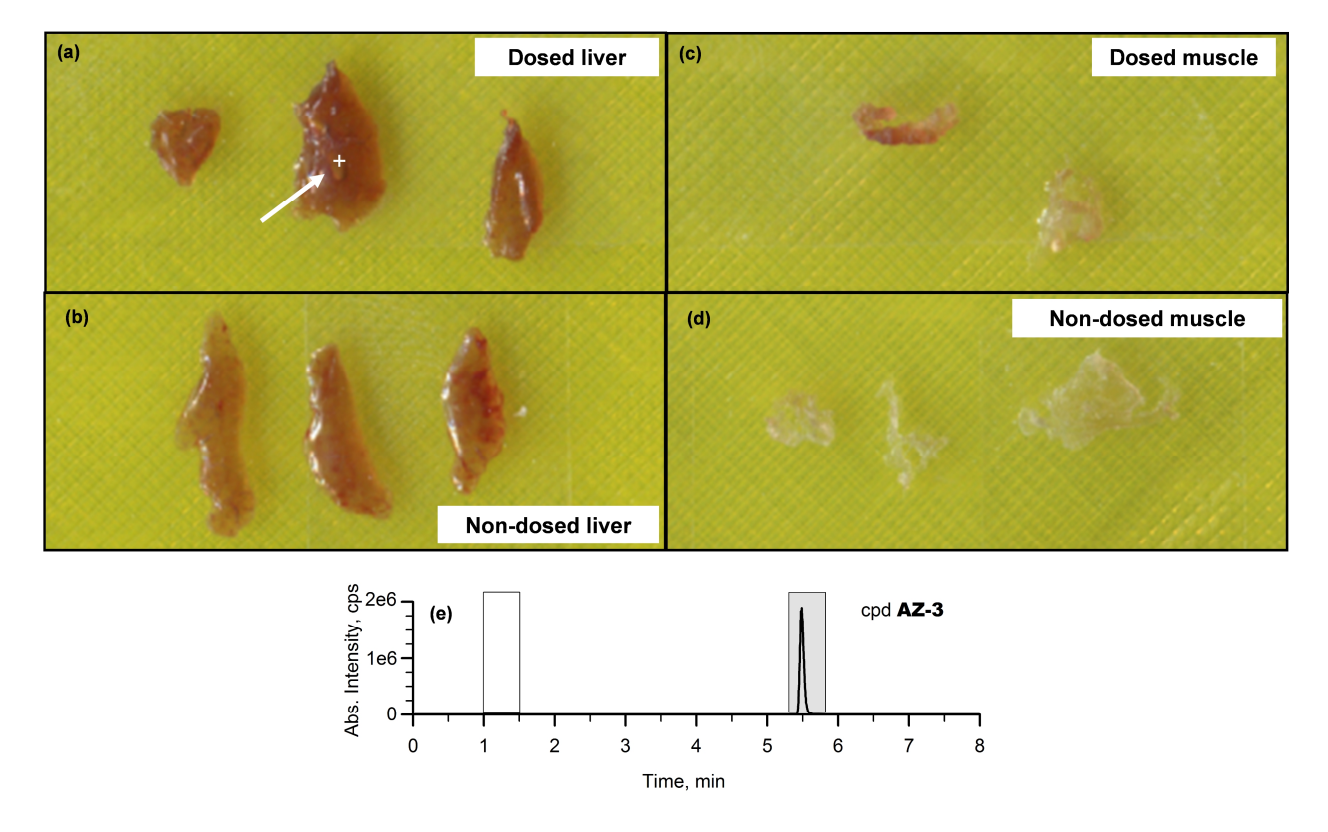


Figure S5. Magnified optical images of (a) liver and (c) muscle samples of a mouse dosed with AZ-3 (50 mg/kg, dosed subcutaneously, sacrificed 2 h after dose) showing a sampled location indicated by the arrow and a "+" sign in (a). Magnified optical images of (b) liver and (d) muscle samples of a non-dosed mouse. (e) Signal level at this sampling spot was recorded during an 8 min HPLC/MS analysis for compound **AZ-3** (m/z 452.1 \rightarrow 172.1). Gray and white sections show the time ranges used for peak integration (R_t =5.3-5.8 min) and background calculation (R_t =1-1.5 min), respectively, when creating a heat map in Figure 4.